Symmetrical Observability of Kinematic Parameters in Symmetrical Parallel Mechanisms

S. Durango[a], D. Restrepo[a], O. Ruiz[a], J. Restrepo-Giraldo[b,§], S. Achiche[b]

[a] *CAD CAM CAE research laboratory, EAFIT University, Medellín, Colombia*

[b] *Management Engineering Dept., Technical University of Denmark, Lyngby, Denmark*

sdurang1@eafit.edu.co, drestr21@eafit.edu.co, oruiz@eafit.edu.co, jdrg@man.dtu.dk[§], soac@man.dtu.dk

[§]*Corresponding author*

August 18, 2010

Abstract

This article presents an application of symmetry group theory in kinematic identification of parallel mechanisms of n_{legs} legs. Kinematic Identification implies the estimation of the actual geometrical parameters (as opposed to nominal ones) of a physical mechanism. For a symmetric mechanism, KI requires configuring sets of leg positions with symmetrical observability. This article presents as main contributions: (*i*) a conjecture that allows mapping the symmetries of the mechanism into the active-joint workspace, (*ii*) a set of necessary conditions to express leg parameters in coordinate systems which allow symmetrical observability, and (*iii*) a procedure for exploiting symmetries in pose selection for kinematic identification of symmetrical parallel mechanisms. For the kinematic identification itself, we adopt a divide-and-conquer (DC) identification protocol -discussed by us in another publication- in which each leg of the mechanism is independently identified by using the inverse calibration method. In this article we emphasize how to exploit the symmetries existent in $(n_{legs} - 1)$ legs of the parallel mechanism allowing to apply to other legs the symmetry-transformed sample protocol used for the kinematic identification of a *reference* leg. The symmetrical observability of sets of leg parameters allows to reduce the costs of the pose selection procedure by a factor of $(1/n_{legs})$ compared to a complete DC procedure in which the poses of each leg are selected independently. The pose selection is carried out only for the reference leg. For the $(n_{legs}-1)$ remaining legs the poses are dictated by symmetry operations performed onto the poses of the reference leg. An application of the symmetrical observability is presented through the simulated kinematic identification of a $3\underline{R}RR$ symmetrical parallel mechanism.

Keywords: Symmetrical observability, kinematic identification, parallel mechanisms.

Glossary

C	Jacobian identification matrix		polygon
D_{2n}	Dihedral group of a n-vertices regular	F	Constraint kinematic equation

G	Group
$L,\ l$	Length of a link
N	Number of identification poses
$\mathbf{Q}$	Column matrix of active-joint configurations
$\underline{Q}$	Q matrix of a QR decomposition
$\mathbf{P}$	Column matrix of parametric representations of the end-effector orientation
$\mathbf{R}$	Column matrix of end-effector position vectors
$\underline{R}$	R matrix of a QR decomposition
$\underline{R}RR$	Revolute – revolute – revolute kinematic structure
V	Polygon
g	Inverse kinematic equation
k	Gain of an active-joint sensor
n_{DOF}	Number of degrees of freedom
n_{legs}	Number of legs of a parallel mechanism
n_{φ}	Number of parameters to be identified
q	Active joint variable
$\mathbf{q}$	Vector of active joint variables
$\mathbf{r}$	Position vector
s	Singular value

Greek symbols

Σ	Symmetry group
α, β	Planar angles
γ	Offset of an active-joint sensor
φ	Set of kinematic parameters of a parallel mechanism
λ	Symmetric operation
θ	Active-joint angle
ρ	Parametric representation of the end-effector orientation, *e.g.* a set of Euler angles
σ	Standard deviation
ψ	Reading of an active-joint sensor

Subscripts

$_C$	Symmetrical observability
$_M$	Mechanism
$_Q$	Active joints
$_W$	Workspace
$_i$	Indexing variable
$_\kappa$	κth leg of a parallel mechanism

Superscripts

^{T}	Transpose
^{j}	jth pose of the mechanism

1 Introduction

Parallel mechanisms are instances of closed-loop mechanisms typically formed by a moving platform connected to a fixed base by several legs. Most of parallel mechanisms are formed by a symmetrical structure. Symmetrical parallel mechanisms are defined in the following manner, [1, 2]:

1. the number of legs equals to the number of degrees of freedom of the mechanism,

2. each leg is controlled by one actuator,

3. each leg is formed by an identical kinematic chain, and

4. in at least one particular configuration the kinematic structure defines a symmetry group G_M.

Structural symmetries had been used for workspace and singularity analyses of symmetrical parallel mechanisms, [1, 2, 3] – [3, 4]. With this article we extend the use of structural symmetries addressing the problem of configuring symmetrically observable sets of leg parameters. The necessary conditions to configure symmetrically observable sets is developed in section 5. A main condition is the workspace symmetry that was probed for symmetrical parallel mechanisms in [1, 2]. If a linear model with joint gain and offset is assumed for the active joints, then the active-joints workspace symmetry is required too. The proof of an active-joints symmetrical workspace theorem is analogous to the forward kinematics problem of parallel mechanisms that in general has only numerical solution, [5]. In consequence, a conjecture for the active-joint workspace symmetry is proposed in section 4.

A natural use for the symmetrical observability would be a divide-and-conquer (DC) kinematic identification in which the identification experiments are planed for a reference leg only and extended to the remaining legs by symmetrical operations. For kinematic identification we update the DC protocol, [6], with a symmetrical pose selection procedure, section 5.1.

The layout for the rest of the article is in the following manner: Section 2 develops a literature review in application of symmetries in parallel mechanisms analysis. Section 3 presents fundamentals of symmetry groups theory. A theorem of symmetrical workspace of symmetrical parallel mechanisms is extended on section 4 proposing a conjecture for symmetrical active-joints workspace. The symmetrical observability of sets of leg parameters is proposed in section 5, and its application in symmetrical pose selection for kinematic identification is presented in section 5.1. Results are presented in section 6 through a $3\underline{R}RR$ parallel mechanism case study in which an application of symmetrical observability of sets of leg parameters is used in a simulated kinematic identification. Finally, concluding remarks are presented in section 7.

2 Literature review

Structural symmetries are a common characteristic of most of parallel mechanisms, [2]. However, the analysis of the symmetrical characteristics of parallel mechanisms is one of the least-studied problems. Literature is restricted to workspace and singularity analyses.

Reference [1] presents a symmetric theorem of workspace for symmetrical parallel mechanisms. The theorem reveals an analogous relationship between the workspace shape and the symmetrical structure. This theorem is proposed to estimate geometry characteristics of the workspace and to guide the conceptual design of spatial parallel manipulators. The theorem is limited to mechanisms in which each identical kinematic chain (leg) always remains collinear. In [2] the symmetrical workspace theorem is strengthened to include a general category of symmetrical parallel mechanisms in which the permanent collinearity of the legs is not required. Reference [4] presents an application of the symmetrical workspace theorem that addresses the symmetrical calculation of singularities of symmetrical parallel mechanisms. A common characteristic of [2, 4] is the use of symmetry groups theory for proving the symmetrical theorems. Different from [1, 2, 4], [3] presents a methodology based in a parametric representation of the orientation for the workspace and singularity symmetrical analyses of spherical parallel mechanisms.

This article extends the use of structural symmetries in parallel mechanisms addressing the problem of configuring symmetrically observable sets of leg parameters. Symmetrical observability has direct application in kinematic identification by means of the symmetrical planning of independent identification experiments for each leg. We update the DC protocol, [6], with a symmetrical pose selection procedure. With respect to traditional identification methods the protocol has reported the following advantages:

1. the identification poses are optimized for the identification of reduced sets of parameters (the sets corresponding to each leg),

2. the independent identification of the set of parameters of each leg improves the numerical efficiency of the identification algorithms, and

3. by (1) and (2) calibrating the kinematic model with the identified set of parameters results in a better end-effector accuracy with respect to calibrations by means of other traditional kinematic identification methods.

We improve the DC protocol replacing the independent leg pose selection procedure by a symmetrical pose selection procedure, section 5.1. The DC protocol is updated with an additional advantage:

4. the costs reduction in the design of identification experiments by the use of observability symmetries, *e.g.* compared with a DC independent leg pose selection the costs are reduced to $1/n_{legs}$.

Section 3 presents an introduction to symmetry groups theory required for the analysis of workspace, active-joints and observability symmetries.

3 Fundamentals of symmetry groups

A group is a set G equipped with an internal binary operation $\odot$ such that the binary operation is associative, with closure, and has a neutral and an inverse element in G, [7].

We use two instances of groups to describe symmetries of the structure, workspace and observability of parameters in parallel mechanisms: The symmetry group Σ, section 3.1, and the dihedral group D_{2n}, section 3.2.

3.1 Symmetry group Σ

Let V a polygon in the plane. The symmetry group $\Sigma(V)$ consists of all the rigid motions λ for which $\lambda(V) = V$, that is, the symmetry group is formed by the operations that allow the polygon to superimpose with itself, [2].

3.2 Dihedral group D_{2n}

Let V_n denotes a regular polygon with n vertices and center O. The vertices of V_n are denoted as v_i $(i = 1, 2, \ldots, n)$. The symmetry group $\Sigma(V_n)$ is called the dihedral group of V_n with $2n$ elements and denoted as D_{2n}. The elements of the dihedral group depend on the parity of the regular polygon. A complete description of the dihedral group can be founded in [2].

As an example, consider the symmetries of the equilateral triangle shown in Fig. 1. These symmetries can be expressed by the dihedral group D_6 whose elements are permutations of the set of vertices $V = \{v_1, v_2, v_3\}$. In consequence, the symmetrical group is defined by:

$$D_6 = \{\lambda_1, \lambda_2, \lambda_3, \lambda_4, \lambda_5, \lambda_6\}, \tag{1}$$

where $\lambda_1 = (1)$ denotes a 0-rotation about point O, $\lambda_2 = (123)$ denotes a $2\pi/3$-rotation about point O, $\lambda_3 = (132)$ denotes a $4\pi/3$-rotation about point O, $\lambda_4 = (23)$ denotes a reflection about the line Ov_1, $\lambda_5 = (13)$ denotes a reflection about the line Ov_2, and $\lambda_6 = (12)$ denotes a reflection about the line Ov_3, [4].

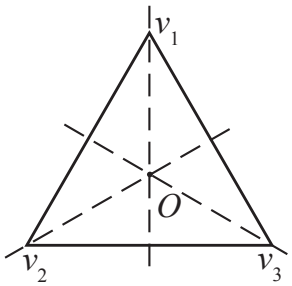

Figure 1: Reflection lines of an equilateral triangle, [4].

Symmetry groups theory is used by [2] to prove the symmetrical theorem of workspace for symmetrical parallel mechanisms. The theorem is summarized in section 4.1.

4 Symmetrical active-joints workspace of symmetrical parallel mechanisms

The workspace of a parallel mechanism is defined as the total volume swept out by the end-effector as the mechanism executes all possible motions, [8]. A symmetrical theorem of workspace for symmetrical parallel mechanisms was proposed by [2] in the following manner:

4.1 Theorem. Symmetrical workspace of symmetrical parallel mechanisms

If the symmetry group of the workspace of a mechanism is denoted by G_W and the symmetry group of the kinematic chain structure being the end-effector in a particular configuration is denoted by G_M, then G_M must be a subgroup of G_W, namely, the following relation always hold:

$$G_M \subseteq G_W. \tag{2}$$

In consequence, if the kinematic structure of a mechanism has associated a symmetry group G_M, then the end-effector workspace G_W remains unaltered under the symmetry operations λ that are the elements of G_M.

A proof of the symmetrical theorem of workspace is provided in [2] using symmetry groups theory.

The workspace symmetry is a necessary condition to configure symmetrically observable sets of leg parameters, section 5. If a linear model with gain and offset is assumed for the active joints, then a symmetrical active-joints workspace is required too, section 5.

In section 4.2 we extend the workspace symmetries to the active-joints workspace of symmetrical parallel mechanisms.

4.2 Conjecture. Symmetrical active-joints workspace of symmetrical parallel mechanisms

In practice, most parallel mechanisms have symmetric structure and a correspondent symmetrical workspace, [1, 2]. However, a symmetrical workspace is not a sufficient condition to obtain a correspondent symmetrical active-joints workspace. We propose a symmetrical conjecture of active-joints workspace for symmetrical parallel mechanisms in the following manner:

> If a symmetrical parallel mechanism has a symmetrical end-effector workspace characterized by a symmetry group G_W, then its is possible to configure a reference system for the active-joint variables that produces a symmetrical active-joints workspace characterized by a symmetry group G_Q.

The conditions to configure a symmetrical parallel mechanism with symmetrical workspace are summarized in the following manner:

1. The number of legs is equal to the number of degrees of freedom of the mechanism.

2. All the legs have an identical structure. This is, each leg has the same number of active and passive joints and the joints are arranged in an identical pattern.

3. The constraint kinematic equation of each leg of the mechanism, F_κ, can be expressed in its implicit form:

$$F_\kappa = g_\kappa(\varphi_\kappa, \mathbf{r}, \rho) - q_\kappa = 0 \qquad (\kappa = 1, 2, \cdots, n_{legs}) \tag{3}$$

where κ denotes the κth leg, g_κ is an inverse kinematic function, φ_κ is the set of kinematic parameters, $\mathbf{r}$ is the position vector of the end-effector, ρ is a parametric representation of the platform orientation (*e.g.* a set of Euler angles), and q_κ is the active-joint variable. The set of

constraint equations for the complete mechanism is defined in the following manner:

$$F(\mathbf{q}) = \begin{bmatrix} F_1(q_1) \\ F_2(q_2) \\ \vdots \\ F_{n_{limbs}}(q_{n_{limbs}}) \end{bmatrix} = \begin{bmatrix} g_1(\varphi_1, \mathbf{r}, \rho) - q_1 \\ g_2(\varphi_2, \mathbf{r}, \rho) - q_2 \\ \vdots \\ g_{n_{limbs}}(\varphi_{n_{limbs}}, \mathbf{r}, \rho) - q_{n_{limbs}} \end{bmatrix}. \tag{4}$$

where $\mathbf{q} = [q_1 \; q_2 \; \cdots q_{n_{legs}}]^T$ is the vector of active joint variables.

4. The kinematic structure of the mechanism has associated a symmetry group G_M in a particular configuration of the end-effector.

Additionally to the conditions of the symmetrical mechanism and symmetrical workspace, we assume the following condition to configure a symmetrical active-joints workspace:

5. The active-joints reference system is defined such that in the particular configuration that defines the symmetry group of the mechanism structure G_M, the active-joints variables are symmetric too. The symmetry group of the active joint variables is denoted as G_Q.

If the active-joints workspace is symmetric the following relation holds:

$$F(\lambda_i(\mathbf{q}) = \lambda_i(F(\mathbf{q})) \qquad (i = 1, 2, \cdots, n_{legs}) \tag{5}$$

where F is the set of constraint kinematic equations of the mechanisms, Eq. 4 and $\lambda_i \in G_Q$ is a symmetry operation of the active-joints workspace symmetry group.

The proof of Eq. 5 is analogous to the forward kinematics of parallel mechanisms: it requires the solution of the constraint kinematic equations given the vector of joint variables. In general it is not possible to express the forward kinematics of parallel mechanisms in an analytical manner, [5]. In consequence, a proof of the symmetrical conjecture of active-joints workspace is not straightforward. We will not provide an analytical proof of the conjecture. However, in section 6 we validate

the conjecture with the numerical analysis of the workspace and active-joints workspace of a three-degrees-of-freedom parallel mechanism formed by revolute joints only.

In section 5 the workspace and active joint symmetries are used in the configuration of symmetrical sets of leg parameters with an application in kinematic identification of symmetrical parallel mechanisms.

5 Symmetrical observability of kinematic parameters

If a parallel mechanism mets the conditions of the symmetrical theorem of workspace, section 4.2 and references [1, 2], then it is possible to configure its set of kinematic parameters in order to obtain a symmetrical observability of its legs. In consequence, the planning of the kinematic identification experiments can be reduced according to the observability symmetry group.

In order to configure symmetrically observable sets of leg parameters we assume the following conditions:

1. The symmetries of the mechanism structure are described by the symmetry group G_M.

2. The mechanism has a symmetrical workspace characterized by a symmetry group G_W. The symmetrical theorem of workspace for spatial parallel mechanisms is proposed in [1, 2] and summarized in section 4.1.

3. The geometric method is adopted for the kinematic modeling of the mechanism. An independent vector-loop constraint kinematic equation is written for each leg in the form of Eq. 3. In consequence, the following hypothesis are assumed:

   (a) each U-joint forming a leg is modeled as perfect,

   (b) each spherical joint forming a leg is modeled as perfect,

   (c) each prismatic joint is modeled as perfectly assembled with respect to its neighbor joints (U-joints, spherical joints, revolute joints, etc.),

(d) the axis of each revolute joint is modeled as perfectly orientated,

(e) if the mechanism is planar, then all the links are modeled as constrained in the mechanism plane.

The hypothesis (3a) to (3e) are consequent with realistic operation conditions in which the influences of defects in the joints have a minor effect on pose accuracy compared with errors in the location of the joints, [9].

4. The position of each base fixed point A_κ (U-joint, spheric joint, etc.) is defined by three parameters, Fig. 2:

   (a) the magnitude of the $\overline{OA_\kappa}$ segment $(\kappa = 1, 2, \ldots, n_{legs})$,

   (b) the angle α_κ of the $\overline{OA_\kappa}$ segment with respect to the Z axis of the base reference system, $\kappa = 1, 2, \ldots, n_{legs}$,

   (c) the angle β_κ of the projection of the segment $\overline{OA_\kappa}$ on plane XY with respect to the X axis of the base reference system $(\kappa = 1, 2, \ldots, n_{legs})$.

5. The position of each platform point b_κ (U-joint, spheric joint, etc.) is described by three parameters, defined analogously to the base fixed points, Fig. 2. The $ouvw$ reference system is analogous to the $OXYZ$. The three parameters are denoted as $\overline{ob_\kappa}$, α_{b_κ} and β_{b_κ} $(\kappa = 1, 2, \cdots, n_{legs})$.

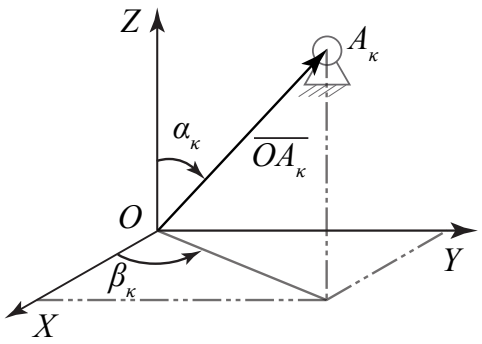

Figure 2: Position of fixed point A_κ

We assume a linear model for the active joints of the mechanism, Eq. 6. In consequence, two additional parameters need to be estimated for each leg: the joint gain k, and the joint offset γ. Therefore, additional symmetry conditions are required to allow a symmetrical observability:

6. Each active joint has the same nominal gain k_κ ($\kappa = 1, 2, \ldots, n_{legs}$).

7. The mechanism has configured a symmetrical active-joints workspace characterized by a symmetry group G_Q. The conditions to configure a symmetrical active-joints workspace are proposed in section 4, conditions (1) to (5).

The linear active-joints model is defined in the following manner:

$$\theta_\kappa = k_\kappa \psi_\kappa + \gamma_\kappa \qquad (\kappa = 1, 2, \cdots, n_{legs}), \tag{6}$$

where θ is the active joint angle, ψ is the sensor reading, k is the gain in the active-joint, and γ is the offset of the sensor.

The symmetrical observability implies that the observability of the ith kinematic parameter of the κth leg in the jth configuration must be the same that the observability of the correspondent parameter of a reference leg in its correspondent symmetrical configuration. The symmetry group of observability, G_C, is defined by the symmetrical operations that allows to superimpose the reference leg with the κth leg. In consequence, the symmetry group G_C can be derived from the symmetry group of the mechanism G_M: $G_C \subseteq G_M$, where

$$G_C = \left\{ \lambda_1, \lambda_2, \ldots, \lambda_{n_{legs}} \right\}. \tag{7}$$

To compute the observability we calculate the observability Jacobian matrix of each leg κ indepen-

dently, namely:

$$
\begin{aligned}
C_\kappa^T &= \begin{bmatrix} (C_\kappa^1)^T & (C_\kappa^2)^T & \cdots & (C_\kappa^N)^T \end{bmatrix} \qquad (\kappa = 1, 2, \ldots, n_{legs}), \\
C_\kappa^j(\varphi_\kappa, \mathbf{r}^j, \rho^j) &= \frac{\partial F_\kappa(\varphi_\kappa, \mathbf{r}^j, \rho^j)}{\partial \varphi_\kappa^T} \qquad (j = 1, 2, \ldots, N),
\end{aligned}
\tag{8}
$$

where the F_κ function is the κth constraint kinematic equation of the set of Eqs. 4, $\mathbf{r}$ is the end-effector position, and ρ is a parametric represention of the end-effector orientation (*e.g.* a set of Euler angles). Each row of the Jacobian matrix C_κ corresponds to an identification configuration of the mechanism. To calculate the observability of the parameters we adopt the QR decomposition of the observability Jacobian matrix (Eq.8) presented in [10]:

$$
\underline{\mathrm{Q}}^T C_\kappa = \begin{bmatrix} \underline{R} \\ \mathbf{0} \end{bmatrix}, \tag{9}
$$

where $\underline{Q}$ is a $N \times N$ orthogonal matrix, $\underline{R}$ is a $n_\varphi \times n_\varphi$ upper triangular matrix, $\mathbf{0}$ is a $(N - n_\varphi) \times n_\varphi$ zero matrix, and n_φ is the cardinality of φ_κ. The observability of the ith parameter is estimated by its correspondent element on the diagonal of the $\underline{R}$ matrix. Therefore, the symmetrical observability for a set of N end-effector poses $\{\mathbf{R}, \mathbf{P}\}$ is stated as:

$$
|\underline{R}_{ii}^\kappa \left(C_\kappa(\varphi_\kappa, \mathbf{R}, \mathbf{P})\right)| = \left|\underline{R}_{ii}^1 \left(C_1\left(\varphi_1, \lambda_\kappa(\mathbf{R}), \mathbf{P}\right)\right)\right| \quad (i = 1, 2, \ldots, n_\varphi) \quad (\kappa = 1, 2, \ldots, n_{legs}), \tag{10}
$$

where, without loss of generality the first leg is assumed as the reference, $\mathbf{R}$ and $\mathbf{P}$ are column matrices of N position vectors and parametric representations of the orientation of the end-effector respectively, and λ_κ is the κth symmetry operation of G_C that is applied individually over each end-effector position in $\mathbf{R}$. The parameters with magnitude near to zero are less observable, and the non-observable parameters are those for which $R_{ii} = 0$.

The natural use of the symmetrical observability is in kinematic identification. In section 5.1 we

propose a procedure to symmetrically design the kinematic identification poses of parallel mechanisms taking advantage of the symmetrical observability.

5.1 Symmetrical pose selection for kinematic identification

By the symmetrical planning of the kinematic identification of parallel mechanisms it is possible to reduce the optimal posture selection to $1/n_{legs}$ of the original searching. We propose the pose selection procedure in the following manner, Fig. 3:

PS1. Calculation of the observability Jacobian matrix. Given the nominal parameters of a reference leg, φ_1, the correspondent constraint kinematic function, F_1, and a representative set of postures of a workspace without singularities, $\{\mathbf{R}, \mathbf{P}\}$, to calculate the observability Jacobian matrix, $C_1^{\mathbf{R}}$:

$$C_1^{\mathbf{R}}(\varphi_1, \mathbf{R}, \mathbf{P}) = \frac{\partial F_1(\varphi_1, \mathbf{R}, \mathbf{P})}{\partial \varphi_1^T}. \tag{11}$$

PS2. Given the observability Jacobian matrix calculated in step (**PS**1) to select an optimal set of postures $\{\mathbf{R}_1, \mathbf{P}_1\}$, for the kinematic identification of the reference leg. To select the poses we adopt the active calibration algorithm developed by Sun and Hollerbach, [11]. The optimized identification set of postures is then defined in the following manner:

$$\begin{gathered} \max_{\{\mathbf{R_1}, \mathbf{P_1}\}} O_1, \\ \text{subject to} : \mathbf{R}_1 \subset \mathbf{R}, \mathbf{P}_1 \subset \mathbf{P}, \end{gathered} \tag{12}$$

were O_1 is an observability index of the Jacobian matrix defined in the following manner:

$$O_1(C_1(\varphi_1, \mathbf{R}_1, \mathbf{P}_1)) = \frac{(s_1\ s_2 \cdots s_{n_1})^{1/n_\varphi}}{n_\varphi}, \tag{13}$$

n_φ is the number of parameters to be estimated, and s_i $(i = 1, 2, \ldots n_\varphi)$ are the singular values of the Jacobian matrix. As a rule of thumb the number of identification poses should be two or

three times larger than the number of parameters to be estimated, [12].

PS3. Given the selected set of identification poses of the reference leg, $\{\mathbf{R1}, \mathbf{P1}\}$, calculated in step (**PS**2) and the observability symmetry group, G_C, to find the sets of identification poses of the remaining $(n_{legs} - 1)$ legs:

$$\begin{aligned} \mathbf{R}_\kappa &= \lambda_\kappa(\mathbf{R_1}) \qquad (\kappa = 2, \ldots, n_{legs}), \\ \mathbf{P}_\kappa &= \mathbf{P_1} \qquad (\kappa = 2, \ldots, n_{legs}). \end{aligned} \tag{14}$$

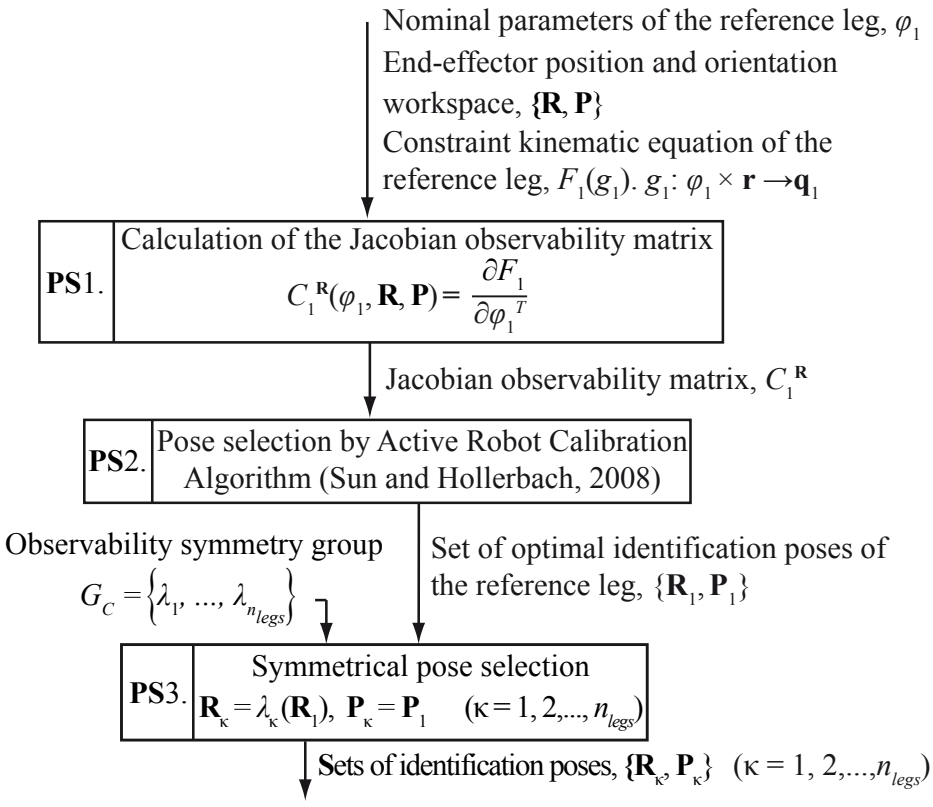

Figure 3: Symmetrical pose selection for kinematic identification

In section 5.2, we update the DC identification protocol, [6], with the symmetrical pose selection procedure.

5.2 Divide-and-conquer identification protocol

The protocol has three main steps that are summarized in the following manner, Fig. 4:

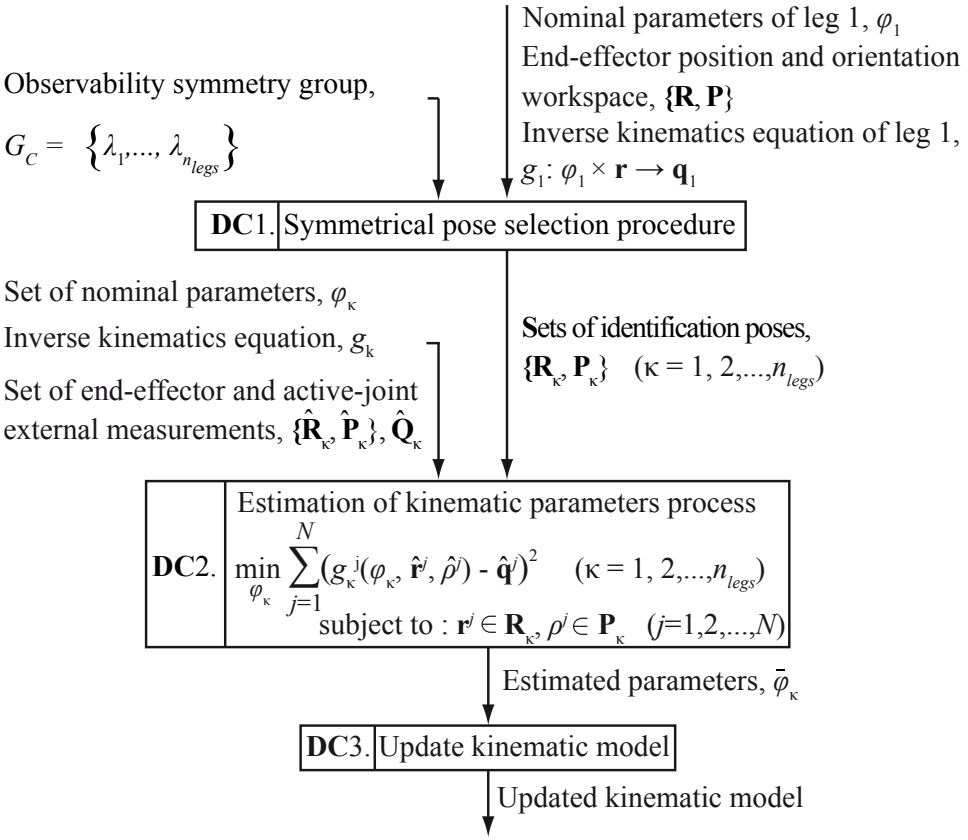

Figure 4: Divide-and-conquer kinematic identification of parallel mechanisms protocol with symmetrical pose selection.

DC1. Symmetrical pose selection. Given the sets of nominal parameters, φ_κ, the inverse kinematic functions, g_κ, and a representative set of postures of a workspace without singularities, $\{\mathbf{R}, \mathbf{P}\}$, to find the independent sets of identification postures, $\{\mathbf{R}_\kappa, \mathbf{P}_\kappa\}$ that maximizes the observability of φ_κ $(\kappa = 1, 2, \ldots, n_{legs})$. Compared to [6], we propose a pose selection that takes advantage of the observability symmetries: the identification poses are optimized for a reference leg and the remaining $n_{legs} - 1$ sets are calculated by symmetry operations. The pose selection procedure is detailed in section 5.1.

DC2. Estimation of kinematic parameters. Given the optimized set, $\mathbf{R}_\kappa, \mathbf{P}_\kappa$, of identification poses obtained in (**DC**1), the correspondent sets of active joint measurements, $\hat{\mathbf{Q}}_\kappa = \left[\hat{q}_\kappa^1 \ \cdots \ \hat{q}_\kappa^N\right]^T$, and end-effector measurements, $\{\hat{\mathbf{R}}_\kappa, \hat{\mathbf{P}}_\kappa\}$, to solve the optimization problem defined in Eq. 15 for the estimation of the sets of kinematic parameters φ_κ $(\kappa = 1, 2, \ldots, n_{legs})$. The opti-

mization problem is defined in the following manner:

$$\begin{aligned} &\min_{\varphi_\kappa} \sum_{j=1}^{N} \left(g_\kappa^j(\varphi_\kappa, \hat{\mathbf{r}}^j, \hat{\rho}^j) - \hat{q}_\kappa^j \right)^2 \qquad (\kappa = 1, 2, \ldots, n_{legs}), \\ &\text{subject to} : \mathbf{r}^j \in \mathbf{R}_\kappa, \rho^j \in \mathbf{P}_\kappa \qquad (j = 1, 2, \ldots, N), \end{aligned} \tag{15}$$

where $\mathbf{R}_\kappa \subset \mathbf{R}, \mathbf{P}_\kappa \subset \mathbf{P}\}$. $\{\mathbf{R}, \mathbf{P}\}$ is a workspace without singularities constraining the optimization problem.

DC3. Update of kinematic model. Given the identified sets of parameters obtained in (**DC**2) to update the kinematic model of the parallel mechanism.

Section 6 presents the study of workspace, active-joints workspace and observability symmetries applied in the kinematic identification of a $3\underline{R}RR$ symmetrical parallel mechanism.

6 Results

The application of symmetries in the kinematic identification of symmetrical parallel mechanisms is presented through a $3\underline{R}RR$ symmetrical parallel mechanism case study. The mechanism has three degrees of freedom and is illustrated in Fig. 5. It consists on an equilateral moving platform, $b_1b_2b_3$, that is connected by three identical revolute – revolute – revolute ($\underline{R}RR$) kinematic chains, $A_\kappa C_\kappa b_\kappa$ ($\kappa = 1, 2, 3$), to an equilateral fixed base, $A_1A_2A_3$, Fig. 5a. Each kinematic chain is actuated from an active-joint that is located on the fixed base. The following set of nominal parameters is assumed:

1. Dimensions of the links: $A_1A_2 = A_2A_3 = A_1A_3 = 6.00$ m, $b_1b_2 = b_2b_3 = b_1b_3 = 1.50$ m, $l = L = 1.50$ m.

2. Configuration of the legs (dyads): $[-1 \ -1 \ -1]$. Each leg is be considered as a dyad that can be configured $+1$ or -1 according to the convention described in Fig. 5.

3. Nominal gain in the active-joint sensors: $k_1 = k_2 = k_3 = 1$.

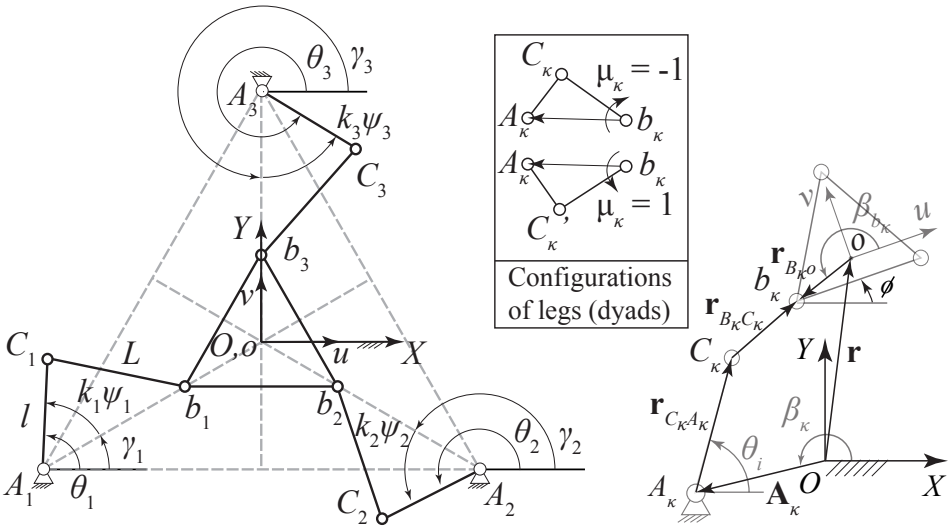

a. Mechanism in symmetric configuration b. Kinematic loop of the κth leg

Figure 5: $3\underline{R}RR$ symmetrical parallel mechanism. Kinematic parameters and constraint loop. Kinematic parameters: $\varphi_\kappa = \left[l_\kappa, L_\kappa, \overline{OA}_\kappa, \beta_\kappa, \overline{ob}_\kappa, \beta_{b_\kappa}, k_\kappa, \gamma_\kappa\right]^T$.

For the kinematic modeling, symmetry analysis and kinematic identification we assume that the origin of the fixed coordinate frame is located at the geometric center of the fixed base $A_1A_2A_3$. The X-axis points along the direction of A_1A_2 and the Y-axis is perpendicular to A_1A_2, Fig. 5a. A moving frame is attached to the geometric center of the platform. The u-axis of the platform frame points along the line b_1b_2, and the v-axis is perpendicular to b_1b_2, Fig. 5a. The location of the moving platform is specified by the coordinates of the platform center and the orientation angle of the moving frame with respect to the fixed frame in the following manner:

$$\begin{aligned} \mathbf{r} &= [x \;\; y \;\; 0]^T, \\ \rho &= \phi. \end{aligned} \tag{16}$$

6.1 Workspace symmetry

The $3\underline{R}RR$ symmetrical parallel mechanism satisfies the workspace symmetry conditions (1) to (4), section 4:

1. The mechanism has three legs and three correspondent degrees-of-freedom.

2. Each leg of the mechanism has an identical $\underline{R}RR$ kinematic structure.

3. The constraint kinematic equation of each leg is expressed by a closed loop in the following manner, Fig. 5b :

$$\|\mathbf{r} - \mathbf{A}_\kappa\| - \|\mathbf{r}_{C_\kappa A_\kappa} + \mathbf{r}_{BC_\kappa} - \mathbf{r}_{B_\kappa o}\| = 0 \qquad (\kappa = 1, 2, 3). \tag{17}$$

4. The mechanism structure symmetry group, G_M, is stated by inspection, Fig. 5a. The symmetry group G_M is defined in the following manner:

$$G_M = \{\lambda_1, \lambda_2, \lambda_3, \lambda_4, \lambda_5, \lambda_6\}, \tag{18}$$

where the first three elements of G_M represent rotations about the Z-axis: 0 rad, $2\pi/3$ rad, and $4\pi/3$ rad, and the last three elements of G_M denote reflections about OA_1, OA_2, and OA_3 respectively.

The actuation of the symmetrical group G_M on the end-effector workspace will make the workspace superimpose with itself. The symmetrical workspace theorem for this mechanism is proved on references [1, 2].

6.2 Active-joint workspace symmetry

We assume a linear active-joints model, for the $3\underline{R}RR$ symmetrical parallel mechanism, Eq. 6 with $n_{legs} = 3$. In consequence, to design a symmetrical kinematic identification is also necessary to satisfy the condition (5) of active-joints workspace symmetry, section 4. Figure 5a presents the symmetrical configuration of the $3\underline{R}RR$ mechanism that determines the symmetry of the active-joints workspace, being the active-joint variables vector defined as $\mathbf{q} = [\psi_1\ \psi_2\ \psi_3]^T$. The mechanism is configured symmetrically positioning the active-joints measuring system in the following manner, Fig. 5a:

$$\gamma_1 = \pi/6 \text{ rad},\ \gamma_2 = 5\pi/6 \text{ rad},\ \gamma_3 = -\pi/2 \text{ rad}. \tag{19}$$

A numerical calculation of the active-joints workspace is performed to validate the symmetrical conjecture, Fig. 6a. Additionally, three constant orientation workspaces are evaluated: $\phi = 0$ rad, $\phi = 0.4$ rad, $\phi = 0.6$ rad. The results are shown on Figs. 6b to 6d. The symmetry group of the active-joint workspace corresponds to rotations of 0 rad, $2\pi/3$ rad, and $4\pi/3$ rad around the axis $\psi_1 = \psi_2 = \psi_3$, Fig. 6a

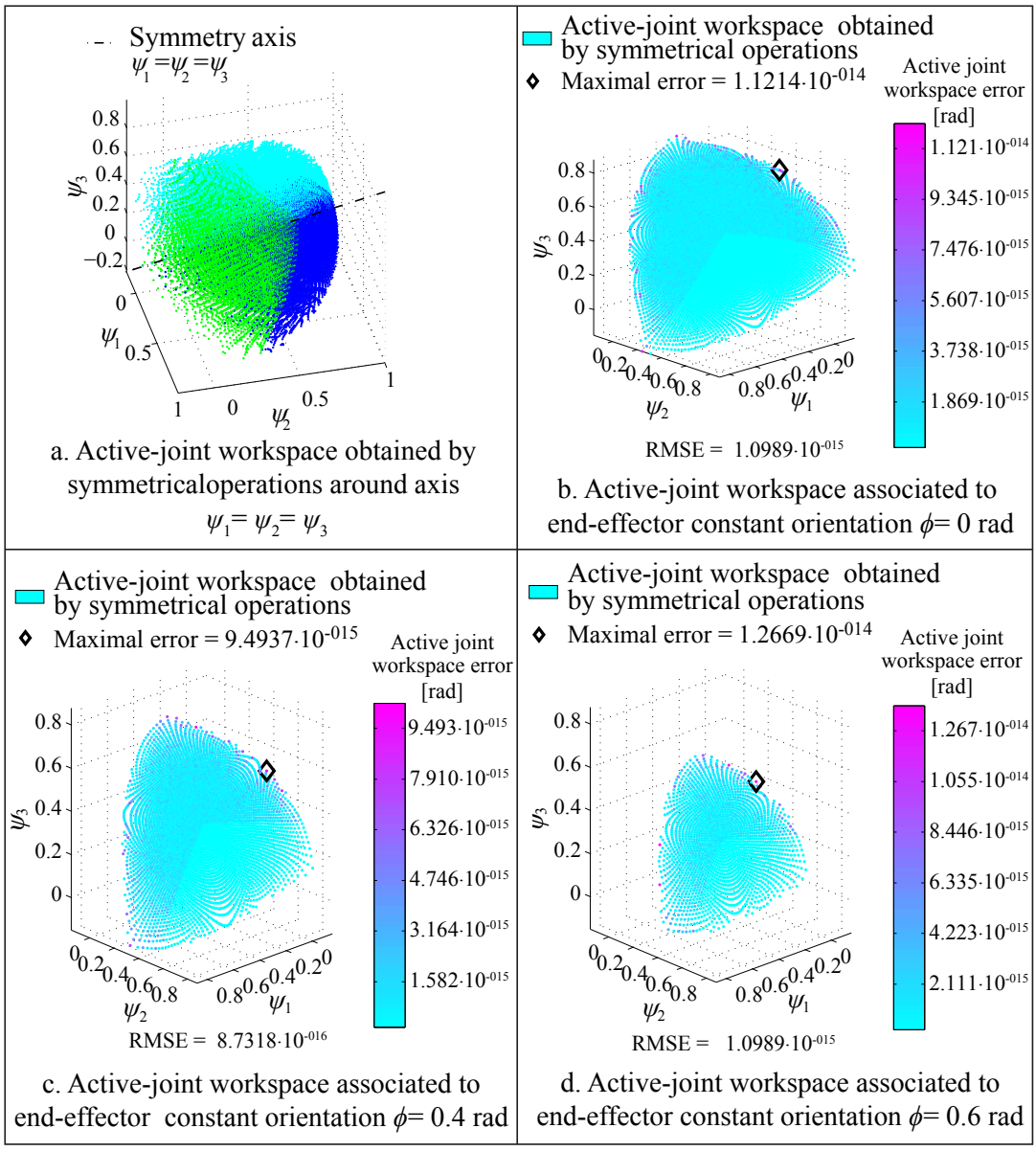

Figure 6: $3\underline{R}RR$ symmetrical parallel mechanism. Active-joint workspace obtained by symmetrical operations. Kinematic parameters: $\overline{A_1A_2} = \overline{A_2A_3} = \overline{A_1A_3} = 6.00$ m. $\overline{b_1b_2} = \overline{b_2b_3} = \overline{b_1b_3} = 1.50$ m, $l = L = 1.50$ m, $k_1 = k_2 = k_3 = 1.00$. Dyads configuration $[-1\ -1\ -1]$.

6.3 Configuration of symmetrically observable sets of leg parameters

Nominally, the set of kinematic parameters is defined by the position of base fixed points, $\mathbf{A}_\kappa$, the position of platform points, $\mathbf{b}_\kappa$, the leg lengths, l_κ and L_κ, and the joint gain and offset, k_κ and ψ_κ $(\kappa = 1, 2, 3)$. Consequently with the conditions (1)–(7) of symmetrical observability, section 5, we configure this set of parameters to be symmetrically observable: The base and platform points are modeled as constrained on the mechanism plane, the fixed base and platform points are defined by the magnitude of the $\overline{OA_\kappa}$ and $\overline{ob_\kappa}$ segments, and the angles β_κ and β_{b_κ} respectively, Fig. 5. A linear model is assumed for the active joints, Eq .6. In consequence, the set of parameters to be identified is defined in the following manner, Fig. 5:

$$\varphi_\kappa = \left[l_\kappa, L_\kappa, \overline{OA_\kappa}, \beta_\kappa, \overline{ob_\kappa}, \beta_{b_\kappa}, k_\kappa, \gamma_\kappa\right]^T \qquad (\kappa = 1, 2, 3) \tag{20}$$

The symmetry observability group, $G_C \subseteq G_M$, corresponds to the symmetry operations that allows the leg 1 to superimpose with the κth leg $(\kappa = 1, 2, 3)$:

$$G_C = \{\lambda_1, \lambda_2, \lambda_3\} \qquad (G_C \subseteq G_M), \tag{21}$$

where G_M is the symmetry group of the mechanism, Eq. 18.

6.4 Symmetrical pose selection for kinematic identification

We adopt the DC identification protocol, section 5.2. The mechanisms meets the symmetry requiered symmetry conditions:

1. the mechanism is symmetric as is probed in sections 6.1 and 6.2, and

2. the sets of leg parameters are configured to obtain a symmetrical observability and the correspondent symmetry observability group is defined, Eqs. 20–21, section 6.3.

Prior to perform the kinematic identification we apply the symmetrical pose selection for kinematic identification procedure, section 5.1:

PS1. Calculation of the identification matrix, $C_1^{\mathbf{R}}(\varphi_1, \mathbf{R}, \mathbf{P})$, Eq. 11. The nominal set of parameters, φ_1, is given by the set of conditions (1) – (3), section 6, the inverse kinematic function, g_1, is given by the Eq. 17 with $\kappa = 1$, and the useful workspace, $\{\mathbf{R}, \mathbf{P}\}$, is given by a set of 30 000 singularity-free configurations of the mechanism.

PS2. Selection of optimal identification poses. A set of 24 optimal identification poses, $\{\mathbf{R}_1, \mathbf{P}_1\}(C_1^{\mathbf{R}})$ is selected using the robot calibration algorithm of of Sun and Hollerbach, [11]. The optimized identification poses are registered in Fig. 7.

PS3. Symmetrical pose selection. The optimal sets of identification poses for the second and third legs are obtained by symmetry operations over the set $\{\mathbf{R}_1, \mathbf{P}_1\}$:

$$\begin{aligned} \mathbf{R}_\kappa &= \lambda_\kappa(\mathbf{R}_1) \qquad (\kappa = 2, 3), \\ \mathbf{P}_\kappa &= \mathbf{P}_1 \qquad (\kappa = 2, 3), \end{aligned} \tag{22}$$

where the symmetry operations, λ_κ are defined by the Eq. 21. In Fig. 8 the symmetrical observability of the legs is verified by the calculation of the observability index, Eq. 10, for the sets of optimal poses.

Once the identification poses are selected, we proceed with the kinematic identification of the mechanism, section 6.5.

6.5 Kinematic identification

The kinematic identification is simulated to evaluate the performance of the improved DC identification protocol. The nominal kinematic parameters of the mechanism are disturbed adding random errors with normal distribution and standard deviation σ in order to simulate the kinematic errors to

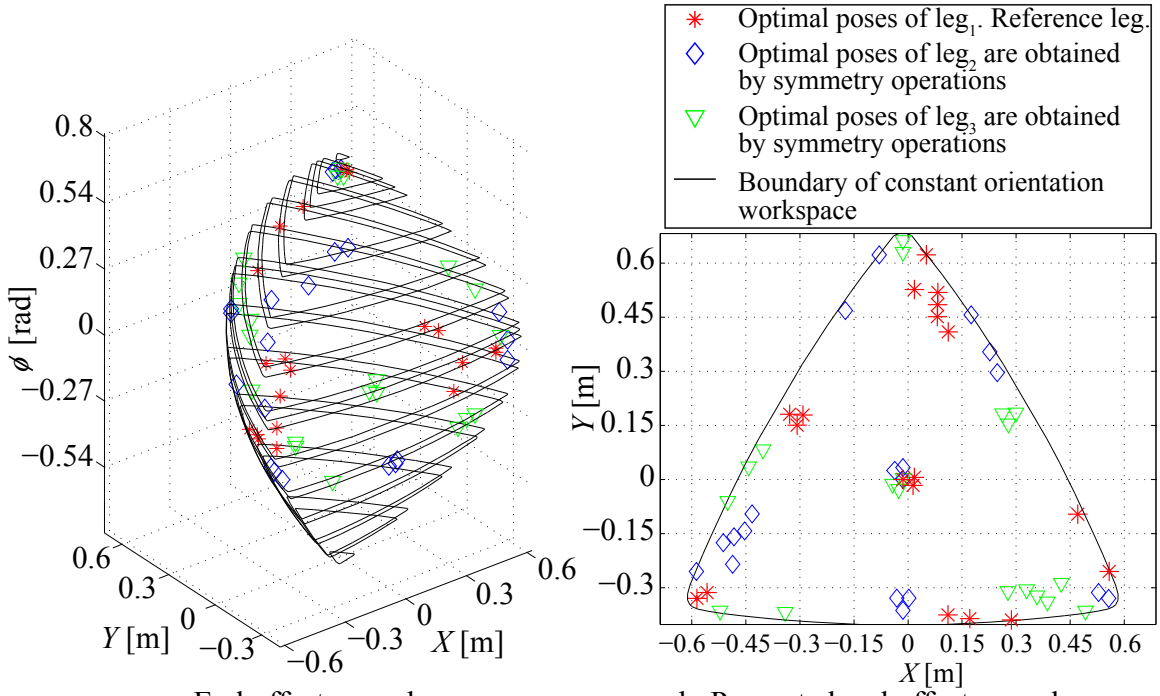

a. End-effector workspace. b. Proyected end-effector workspace.

Figure 7: $3\underline{R}RR$ symmetrical parallel mechanism. Active-joint workspace obtained by symmetrical operations. Kinematic parameters: $\overline{A_1A_2} = \overline{A_2A_3} = \overline{A_1A_3} = 6.00$ m. $\overline{b_1b_2} = \overline{b_2b_3} = \overline{b_1b_3} = 1.50$ m, $l = L = 1.50$ m, $k_1 = k_2 = k_3 = 1.00$. Dyads configuration $[-1\ -1\ -1]$.

be identified. The end-effector measurements, $\hat{\mathbf{R}}_\kappa$, are simulated from its correspondent active-joint measurements, $\hat{\mathbf{Q}}_\kappa$, through a forward kinematics model added with normally distributed random disturbances. For the simulations the standard deviations of the measurements were defined in the following manner:

$$\begin{aligned} \sigma_r &= 1.00 \cdot 10^{-4} \text{ m}, \\ \sigma_\rho &= 1.00 \cdot 10^{-4} \text{ rad}, \end{aligned} \tag{23}$$

where σ_r and σ_ρ are the standard deviations in length and orientation measurements respectively. The identification procedure is as summarized:

DC1. Symmetrical pose selection. The symmetrical pose selection is detailed in section 6.4.

DC2. Estimation of kinematic parameters. A linearization of the inverse kinematics is used for solve the non-linear optimization problem of each leg, Eq. 15. The linearization is defined in the

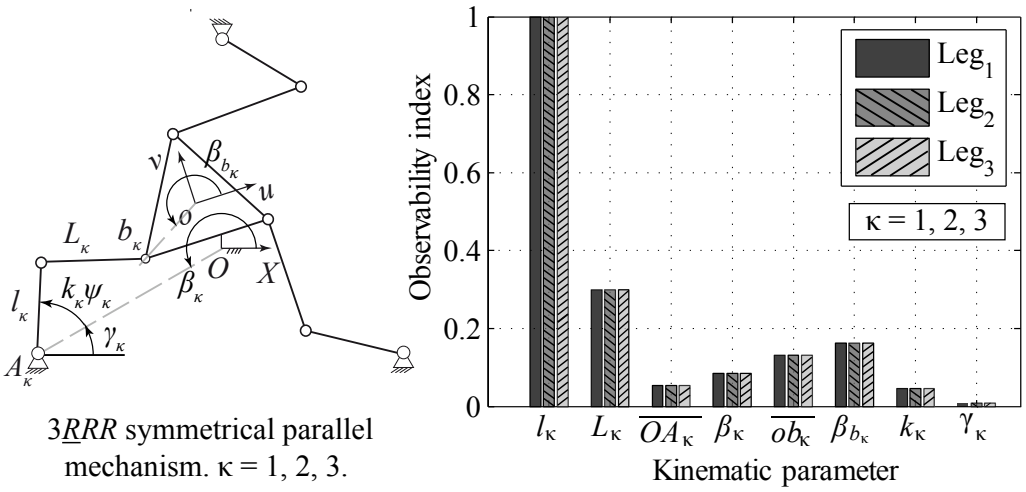

Figure 8: $3\underline{R}RR$ symmetrical parallel mechanism. Active-joint workspace obtained by symmetrical operations. Kinematic parameters: $\overline{A_1A_2} = \overline{A_2A_3} = \overline{A_1A_3} = 6.00$ m. $\overline{b_1b_2} = \overline{b_2b_3} = \overline{b_1b_3} = 1.50$ m, $l = L = 1.50$ m, $k_1 = k_2 = k_3 = 1.00$. Dyads configuration $[-1\ -1\ -1]$.

following manner:

$$\Delta\mathbf{Q}_\kappa = C_\kappa(\varphi_\kappa, \mathbf{R}_\kappa, \mathbf{P}_\kappa)\Delta\varphi_\kappa \qquad (\kappa = 1, 2, 3), \tag{24}$$

where $\Delta\mathbf{Q}_\kappa = \mathbf{Q}_\kappa(\varphi_\kappa, \hat{\mathbf{R}}_\kappa, \hat{\mathbf{P}}_\kappa) - \hat{\mathbf{Q}}_\kappa$ is the error in the active joint variables and $\Delta\varphi_\kappa$ is the set of parameters to be estimated. The estimation is achieved using a iterative linear least-squares solution of Eq. 24:

$$\Delta\varphi_\kappa = (C_\kappa^T C_\kappa)^{-1} C_\kappa^T \Delta\mathbf{Q}_\kappa \qquad (\kappa = 1, 2, 3). \tag{25}$$

DC3. Update the kinematic model with the set of estimated parameters $\overline{\varphi} = \{\overline{\varphi}_1, \overline{\varphi}_2, \overline{\varphi}_3\}$ where

$$\overline{\varphi}_\kappa = \varphi_\kappa + \Delta\varphi_\kappa \qquad (\kappa = 1, 2, 3). \tag{26}$$

The performance of the identification is evaluated after the kinematic calibration by means of the calculation the root mean square (RMSE) of the difference between the commanded end-effector pose, $\{\mathbf{R}, \mathbf{P}\}$, and a correspondent set of simulated measurements, $\{\hat{\mathbf{R}}, \hat{\mathbf{P}}\}$. The set of measured poses corresponds to the set of 30 000 poses used to design the identification experiments. An alternative traditional inverse kinematic calibration is performed using 24 poses optimized for the identification

of the complete set of parameters of the mechanism. The set of optimal poses is selected using the same active robot calibration algorithm as in the case of the DC identification. The results are registered in Fig. 9, RMSE of the end-effector pose estimated for the workspace without singularities before and after calibration, and Fig. 10, local end-effector position errors calculated for constant orientation workspaces ($\phi = 0.0$ rad, $\phi = 0.4$ rad, $\phi = 0.6$ rad).

Concluding remarks of the use of observability symmetries in kinematic identification of parallel mechanisms are presented in section 7.

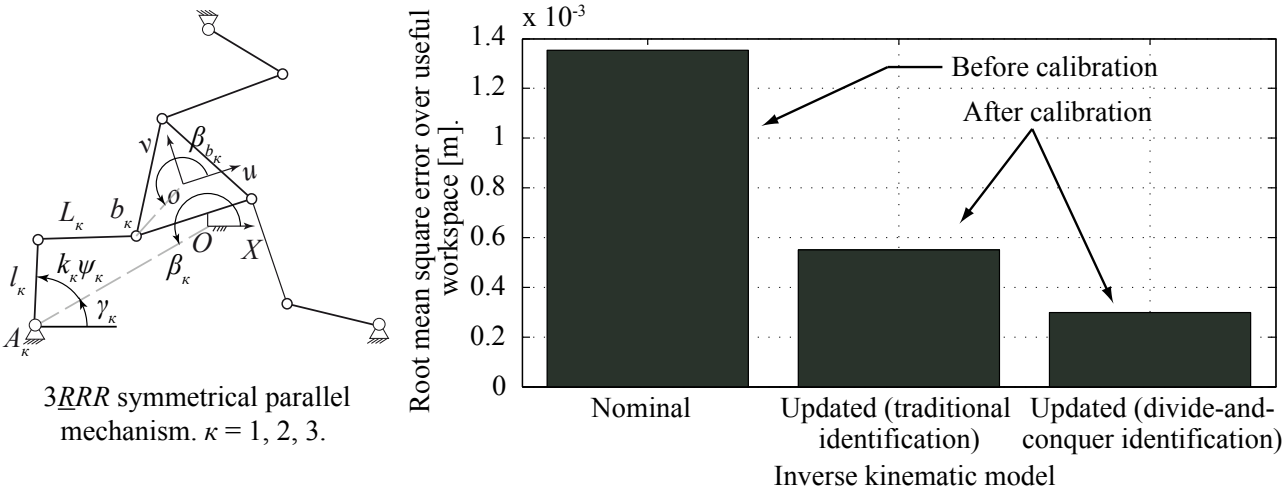

Figure 9: $3\underline{R}RR$ symmetrical parallel mechanism. Estimated root mean square error of the end-effector pose for a workspace free of singularities. $\overline{A_1A_2} = \overline{A_2A_3} = \overline{A_1A_3} = 6.00$ m. $\overline{b_1b_2} = \overline{b_2b_3} = \overline{b_1b_3} = 1.50$ m, $l = L = 1.50$ m, $k_1 = k_2 = k_3 = 1.00$. Dyads configuration $[-1\ -1\ -1]$.

7 Conclusions

This article addresses the problem of configuring sets of leg parameters with symmetrical observability for parallel symmetrical mechanisms. The necessary conditions for the symmetrical observability are proposed in section 5 and summarized in the following manner:

1. The mechanism has a symmetric structure and symmetrical workspace characterized by the symmetry groups G_M and G_W respectively, conditions (1) – (2), section 5.

2. The kinematic joints are modeled as perfectly assembled and in the case of planar mechanisms

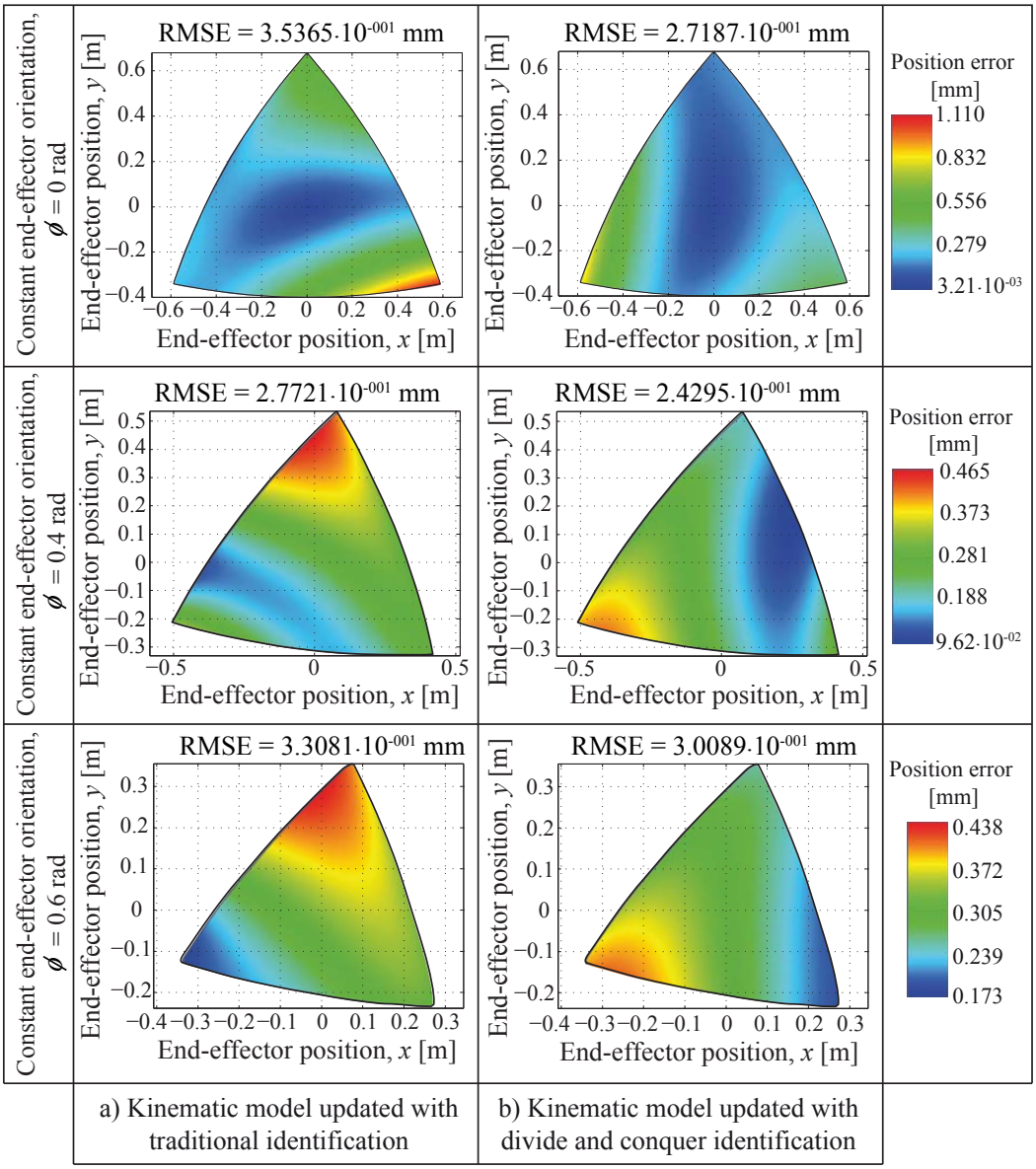

Figure 10: $3\underline{R}RR$ symmetrical parallel mechanism. End-effector position error estimated the constant orientation workspaces. $\overline{A_1A_2} = \overline{A_2A_3} = \overline{A_1A_3} = 6.00$ m, $\overline{b_1b_2} = \overline{b_2b_3} = \overline{b_1b_3} = 1.50$ m, $l = L = 1.50$ m, $k_1 = k_2 = k_3 = 1.00$. Dyads configuration $[-1 \ -1 \ -1]$.

the links are assumed to be constrained in the mechanism plane, condition (3), section 5.

3. The base and platform joint parameters of each leg are defined in order to obtain a symmetrical observability with respect to the workspace, conditions (4) – (5), section 5.

4. If a linear model, Eq. 6, is assumed for the active joints, then additional conditions are required: each active-joint has the same nominal gain and the mechanism has configured a symmetrical active-joints workspace G_Q, conditions (6) – (7), section 5.

To prove the active-joints workspace symmetry results in a problem analogous to the forward kinematics of parallel mechanisms: it requires the solution of the constraint kinematic equations given the vector of input joint variables, Eq. 5. In general it is not possible to formulate an analytical solution of the forward kinematics of parallel mechanisms, [5]. In consequence, we propose the mapping of the structure symmetry to the active-joints workspace symmetry of parallel symmetrical mechanisms as a conjecture, section 4.1.

A natural use for the symmetrical observability would be divide-and-conquer (DC) kinematic identification in which the experiments are designed for a reference leg only and extended to the remaining legs by symmetrical operations. We update the DC protocol, [6], with a new symmetrical pose selection procedure based on the configuration of symmetrically observable sets of leg parameters. Compared with [6], the symmetrical pose selection allows to reduce the design of experiment costs to $1/n_{legs}$. The procedure is developed in section 5.1 and summarized in the following manner:

PS1. Calculation of an observability Jacobian matrix of a singularity-free workspace.

PS2. Selection of set of optimal identification poses of a reference leg. The pose selection is calculated using the active robot calibration algorithm [11] over the observability Jacobian matrix.

PS3. Determination of the optimal poses for the remaining $n_{legs} - 1$ by the symmetrical observability operations over the reference set.

The updated DC kinematic identification protocol is presented in section 5.2. Compared to traditional identification methods the improved protocol has the following advantages:

1. the costs reduction in the design of identification experiments by the use of observability symmetries,

2. the improvement of the numerical efficiency of the procedure for the selection of optimal identification poses by the adoption of the active robot calibration algorithm [11],

3. the reduction of kinematic identification computational costs by the identification of reduced sets of parameters (the sets correspondent with each leg), and

4. as a consequence of (1) – (3), the improvement of the kinematic identification results.

8 Acknowledgments

The authors wish to acknowledge the financial support for this research by the Colombian Administrative Department of Sciences, Technology and Innovation (COLCIENCIAS), and the National Service of Learning of Colombia (SENA), grant 1216-479-22001, and by the Autónoma de Manizales University (UAM).

References

[1] Jing-Shan Zhao, Min Chen, Kai Zhou, Jing-Xin Dong, and Zhi-Jing Feng. Workspace of parallel manipulators with symmetric identical kinematic chains. *Mechanism and Machine Theory*, 41(6):632 – 645, 2006.

[2] Jing-Shan Zhao, Fulei Chu, and Zhi-Jing Feng. Symmetrical characteristics of the workspace for spatial parallel mechanisms with symmetric structure. *Mechanism and Machine Theory*, 43(4):427 – 444, 2008.

[3] I.A. Bonev and C.M. Gosselin. Analytical determination of the workspace of symmetrical spherical parallel mechanisms. *IEEE Transactions on Robotics*, 22(5):1011 –1017, oct. 2006.

[4] Jing-Shan Zhao, Fulei Chu, and Zhi-Jing Feng. Singularities within the workspace of spatial parallel mechanisms with symmetric structures. *Proceedings of the Institution of Mechanical Engineers, Part C: Journal of Mechanical Engineering Science*, 224(2):459–472, 2010.

[5] P. Renaud, A. Vivas, N. Andreff, P. Poignet, P. Martinet, F. Pierrot, and O. Company. Kinematic and dynamic identification of parallel mechanisms. *Control Engineering Practice*, 14(9):1099–1109, 2006.

[6] S. Durango, D. Restrepo, O. Ruiz, J. Restrepo-Giraldo, and S. Achiche. Kinematic identification of parallel mechanisms by a divide and conquer strategy. In *7th International Confer-*

ence on Informatics in Control, Automation and Robotics - ICINCO, volume 2, pages 167–173. SciTePress, 2010.

[7] O. Ruiz and C. Cadavid. *Geometrics Functions in Computer Aided Geometric Design*. Fondo Editorial Universidad EAFIT, first edition, 2008.

[8] B. Siciliano and O. Khatib, editors. *Springer Handbook of Robotics*. Springer, Berlin, 2008.

[9] D. Daney. Kinematic calibration of the gough platform. *Robotica*, 21(06):677–690, 2003.

[10] S. Besnard and W. Khalil. Identifiable parameters for parallel robots kinematic calibration. In *IEEE International Conference on Robotics and Automation – ICRA*, volume 3, 2001.

[11] Yu Sun and J.M. Hollerbach. Active robot calibration algorithm. In *International Conference on Robotics and Automation – ICRA*, pages 1276–1281, May 2008.

[12] J.H. Jang, S.H. Kim, and Y.K. Kwak. Calibration of geometric and non-geometric errors of an industrial robot. *Robotica*, 19(03):311–321, 2001.